Three-body-interaction effects on the phase-transition and high-pressure behavior of divalent-metal oxides

K. N. Jog
Department of Postgraduate Studies and Research in Physics, Rani Durgawati University, Jabalpur 482001, India

Sankar P. Sanyal* and R. K. Singh
Materials Research Laboratory, Department of Physics, Bhopal University, Bhopal 462 026, India
(Received 5 November 1985; revised manuscript received 2 September 1986)

A three-body-interaction potential (TBP) model has been formulated by incorporating the effects of long-range Coulomb and three-body interactions and short-range van der Waals and overlap repulsion, effective up to second neighbors. The three-body interactions arise from the electron-shell deformation when the nearest-neighbor ions overlap. This TBP has been employed for detailed studies of pressure-induced phase-transition and high-pressure behavior of divalent metal oxides. The model has yielded somewhat more realistic predictions of the phase-transition and high-pressure behavior as compared to those derived from the usual two-body potentials based on phenomenological and *ab initio* approaches.

I. INTRODUCTION

In a recent paper,[1] we reported results for the phase-transition and high-pressure behavior of divalent-metal oxides obtained from two model potentials, one formulation by Sangster and Stoneham[2] (model I) and one by Mackrodt and Stewart[3] (model II). In these studies, we found that the results of the simple phenomenological model I were surprisingly more or less identical to those derived from the relatively more sophisticated model II and the modified electron-gas (MEG) model of Cohen and Gordon[4] for the case of MgO and CaO crystals. Recently, Chang and Cohen[5] used the pseudopotential method[6] within the local-density theory[7] (LDT) and predicted the phase transition ($B_1 \rightarrow B_2$) pressure to be 1050 GPa in MgO. This value is much higher than the values ranging from 117 to 372 GPa predicted by other theoretical workers.[1,4,8] Very recently some more efforts have been made to predict the phase transition in MgO. Mehl *et al.*[9] used a general potential linear augmented-plane-wave (LAPW) method and find a phase transition at 500 GPa. Bukowinski[10] has also studied the B_1 and B_2 phases of MgO using a total energy muffin-tin APW program to find a phase transition at 200 GPa. A quasiharmonic calculation of the B_1 phase of MgO, based on electron gas potential, was carried out by Hemley *et al.*[11] However, the experimental measurements of phase transition pressure based on shock-wave[12] and diamond-cell[13] methods reveal that the phase transition ($B_1 \rightarrow B_2$) in MgO is expected to occur beyond 120 and 95 GPa, respectively. In fact, such differences between theory and experiment for structural phase transitions are found not only in the case of MgO (Ref. 14) alone, but in other oxides also. For example, the predicted value of the transition pressure for SrO is nearly 100 GPa, which is higher than its observed value, 36 GPa.[15] A similar but quantitatively smaller discrepancy is also found in the case of CaO by Jeanloz *et al.*[16] Thus, there is an obvious need for further refinements in the available theories to eliminate these deviations.

Besides the above deficiencies in the available theories, it is found that model I, in our earlier work,[1] was originally formulated for the specific purpose of calculating the defect energies which required oversimplifications such as the common oxygen polarizability and interactions for all divalent metal oxides, negligible cation-cation interactions, and the absence of van der Waals terms in the anion-cation potential. This potential, as such is inadequate for high-pressure studies. In contrast, model II in Ref. 1 takes proper account of the van der Waals forces and makes use of the spirit of microscopic approach for the parameter determination. The MEG calculations are also subject to some deficiencies, which as pointed out by Cohen and Gordon[4,17] themselves, are due to neglect of many-body interactions in these studies. Since the interaction system of all these models consists of only two body pairwise additive potentials therefore, they fail to account for the Cauchy violations ($C_{12} \neq C_{44}$), which are significant in almost all the divalent metal ox-

TABLE I. Input data (elastic constants are in GPa and r_0 is in 10^{-1} nm).

Crystals	C_{11}	C_{12}	C_{44}	r_0
MgO	289[a]	88[a]	155[a]	2.106[b]
CaO	226[c]	62[c]	81[c]	2.405[b]
SrO	173[d]	45[d]	56[d]	2.580[b]
BaO	126[e]	36[f]	34[e]	2.761[b]
MnO	223[g]	120[g]	79[g]	2.222[b]
FeO	359[h]	156[h]	56[h]	2.155[b]
CoO	256[i]	144[i]	80[i]	2.133[b]
NiO	270[i]	125[i]	105[i]	2.084[b]

[a]Reference 28.
[b]Reference 29.
[c]Reference 30.
[d]Reference 31.
[e]Reference 32.
[f]Reference 33.
[g]Reference 34.
[h]Reference 35.
[i]Reference 36.

TABLE II. Model parameters of divalent metal oxides.

Crystals	p_{+-}	p_{++} (10^{-1} nm)	p_{--}	b (10^{-19} J)	$f(r_0)$	$f'(r_0)$ (10^{10} m^{-1})	$f''(r_0)$ (10^{20} m^{-2})
MgO	0.276	0.145	0.368	2.193	0.0068	−0.0582	0.3499
CaO	0.319	0.189	0.402	2.013	0.0019	−0.0245	0.1428
SrO	0.337	0.207	0.410	2.087	0.0011	−0.0176	0.1219
BaO	0.362	0.207	0.426	1.658	−0.0049	0.0039	0.0660
MnO	0.303	0.211	0.375	2.826	0.0259	−0.0854	0.2817
FeO	0.297	0.211	0.368	2.762	0.0252	−0.0849	0.2856
CoO	0.280	0.211	0.370	2.582	0.0251	−0.0896	0.3203
NiO	0.275	0.211	0.370	2.468	0.0258	−0.0938	0.3413

ides (DMO). Also, the semiempirical studies[18,19] on lattice dynamics and statics have shown that nonadditive three-body interactions are important in DMO as there occurs appreciable decrease in their nearest-neighbor separations at high pressures involved in the pressure-induced phase transition. Thus, it is evident from the above view points that a realistic model potential for DMO must include the effects of three-body[18−21] and van der Waals interactions. Motivated from these requirements, we have formulated a more realistic three-body potential (TBP) which consists of the long-range Coulomb and three-body interactions (TBI) and short-range overlap repulsion of Hafemeister and Flygare[22] (HF) type, van der Waals dipole-dipole and dipole-quadrupole attractions whose coefficients have been obtained from the Slater-Kirkwood variational (SKV) approach.[23]

The proposed TBP model has been found to give improved results and successful description of the high pressure behavior of DMO. These results in most cases are better than those obtained from microscopic models whose parameters are derived from *ab initio* approach and short-range potential considered effective up to fourth

TABLE III. Phase transition and high-pressure behavior of divalent metal oxides.

Crystals	Models	ΔU (kJ/mole)	Transition pressure P_t (GPa)	Relative change in volume at P_t (%)	Shear Instability (GPa)	Reference
MgO	TBP	191	302	4.0	1310	present
	I	130	172	4.2	295	1
	II	163	202	5.0	765	1
	MEG (YA)	197	372		932	4
	MEG (Wat)	163	256		555	4
	LDT	145	1050	1.8		5
	Expt.		>120			12
CaO	TBP	130	115	4.7	350	present
	I	117	106	4.7	173	1
	II	134	108	5.5	328	1
	MEG (YA)	138	162		537	4
	MEG (Wat)	129	121		342	4
	Expt.		$70+10$	11.0		24
SrO	TBP	111	80	4.7	225	present
	I	114	95	4.0	143	1
	II	117	88	4.5	353	1
	MEG		>136			15
	Expt.		36 ± 4	13.0		15
BaO	TBP	112	105	1.7	245	present
	I	111	86	3.3	113	1
	II	115	85	3.5	373	1
MnO	TBP	90	96	5.2	1000	present
	I	130	166	3.8	258	1
	II	136	122	5.3	363	1
FeO	TBP	103	119	4.4	1280	present
	I	129	158	5.3	283	1
	II	136	128	5.5	340	1
	Expt.		~90	4.0		24
CoO	TBP	103	112	4.8	1050	present
	I	118	119	6.5	270	1
NiO	TBP	113	137	5.0	1360	present
	I	121	133	6.2	298	1

neighbors.[4] Moreover, the inclusion of three-body effects has improved the prediction of phase transition pressure over those revealed from the models I and II, reported in our earlier paper.[1] A comparison of our results obtained from TBP model is, however, difficult in the case of high pressure region because the experimental data are available only for the low-pressure range (0—30 GPa) for hydrostatic compression while the pressure induced phase transition in DMO occur much beyond this limit. For high pressures, the interpretation of the shock-wave experimental data is quite difficult due to uncertain thermodynamic conditions (as mentioned in Ref. 4) and the smallness of the time duration over which the material is actually under high pressure in these experiments, while the theoretical calculations assume isothermal conditions at 0 K. In view of the geophysical, academic and technological importance of the DMO and until the availability of high-pressure data, the present theoretical investigations with this improved TBP model might be of great importance and use in the understanding of the nature of crystal interactions and high-pressure behavior of these oxides. A brief account of the present TBP model and the method of calculations is given in Secs. II and III, respectively. The computed results have been presented and discussed in Sec. IV.

II. MODEL POTENTIAL

The crystal energy of DMO corresponding to the lattice separation r_{ij}, in the framework of TBP is expressed as

$$U(r)=\sum_{i,j}{}' Z_i Z_j e^2 r_{ij}^{-1}+\sum_{i,j,k}{}' Z_i Z_j e^2 r_{ij}^{-1} f(r_{ik})+\sum_{i,j} c_{ij} r_{ij}^{-6} + \sum_{i,j} d_{ij} r_{ij}^{-8}+\sum_{i,j} b\beta_{ij}\exp[(r_i+r_j-r_{ij})/p_{ij}] , \quad (1)$$

where the first term is the long-range Coulomb energy, the second term represents the three-body interaction energy,[17] third and fourth terms represent the van der Waals interaction energies and the last term is the HF form[22] of short-range repulsive energy. The symbols involved in Eq. (1) have their usual meaning, as explained by Singh and Sanyal.[19] Here, the TBI potential has only three basic

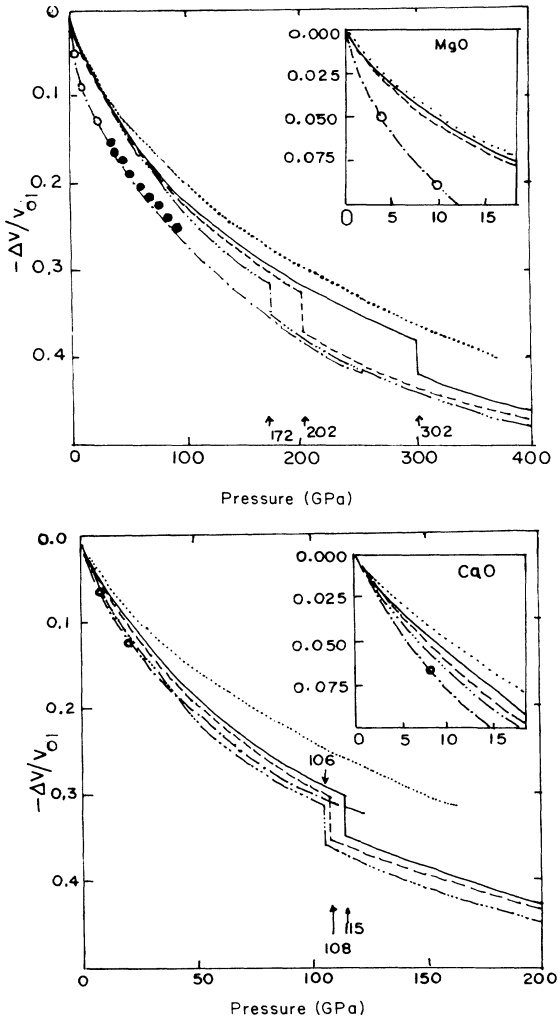

FIG. 1. Phase diagram of MgO and CaO. ——, TBP; — · · · — · · ·, model I; — — —, model II; · · · ·, MEG (YA); —·—·—·, MEG (Wat). Experimental points ○ and ● are taken from Refs. 41 and 13, respectively.

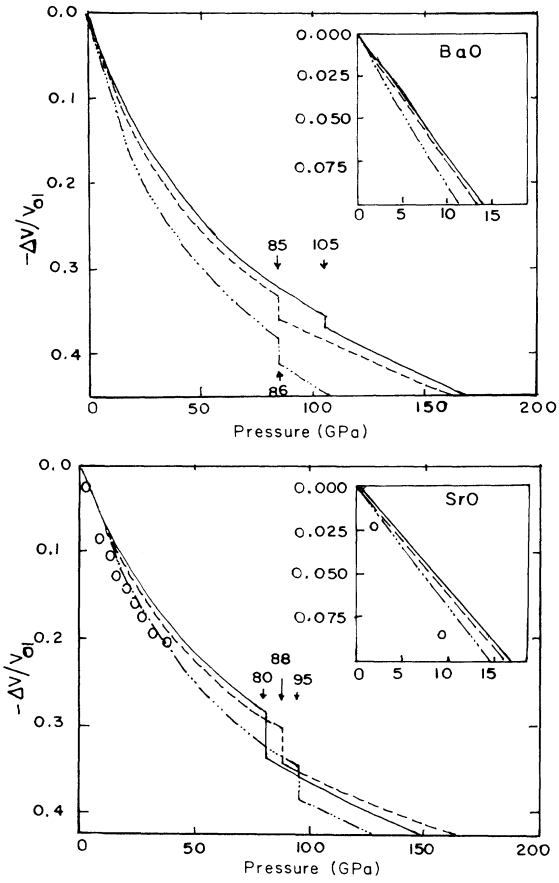

FIG. 2. Phase diagram of SrO and BaO. Other notations are same as in Fig. 1. Experimental points (○) for SrO are taken from Ref. 15.

parameters, e.g., b, p_{ij}, and $f(r)$. We have considered p_{ij} to be different for different ion pairs and used their equilibrium values reported by Mackrodt and Stewart[3] for all DMO except CoO and NiO. The values of p_{+-} for CoO and NiO have been calculated assuming p_{++} and p_{--} to be the same for all transition metal oxides. The values of b and $f(r)$ and its derivatives $f'(r)$ and $f''(r)$ needed for all the oxides are evaluated using the experimental elastic constants and lattice parameter at zero pressure. Also, we have assumed $f(r)$, $f'(r)$, and $f''(r)$ to be the structure-independent parameters. The function $f(r)$ is not expanded in a Taylor series and the sum of the second term in Eq. (1) is cut off beyond first neighbor.[18,19] Moreover, we have not used any input data from its pressure properties which are intended for the prediction in the present study. The input data and model parameters are given in Tables I and II, respectively. The details of the potentials of Models I and II used here for comparison, have been given in Ref. 1 and are not repeated in this paper.

III. METHOD OF CALCULATIONS

The general procedure adopted in the present analysis of relative stability and phase transition of DMO is the same as that in our earlier paper.[1] The values of the energy difference ΔU [$=U(B_2)-U(B_1)$] have been obtained by calculating the cohesive energies $U(B_1)$ and $U(B_2)$ for NaCl (B_1) and CsCl (B_2) phases using the Eq. (1) in its relevant forms at 0 K. The Gibbs free energies $G(B_1)$ and $G(B_2)$ for the two phases at different pressure and corresponding variations of ΔG [$=G(B_2)-G(B_1)$], calculated from the present TBP model has enabled us to determine the phase transition pressure (P_t) at which ΔG becomes zero. The trend of variation of ΔG with pressure is the same as that in the case of models I and II, as reported in our earlier paper,[1] and hence the graphical presentation of variation of ΔG with pressure is avoided in the present paper. The values of ΔU and transition pressures (P_t) thus obtained have been reported in Table III, and compared with the available experimental[12,15,24] and other theoretical[1,4,5] results. In order to make a critical assessment of the success of various theoretical predictions, we have presented the available results of MEG (YA) model,[4] and LDT (based on pseudopotential) model of Chang and Cohen[5] in the same table.

The calculated values of relative volume change $-\Delta V/V_{01}$ (as defined in our earlier paper[1]) have been presented in Table III. The corresponding compression curves (relative volume changes versus pressure) for all

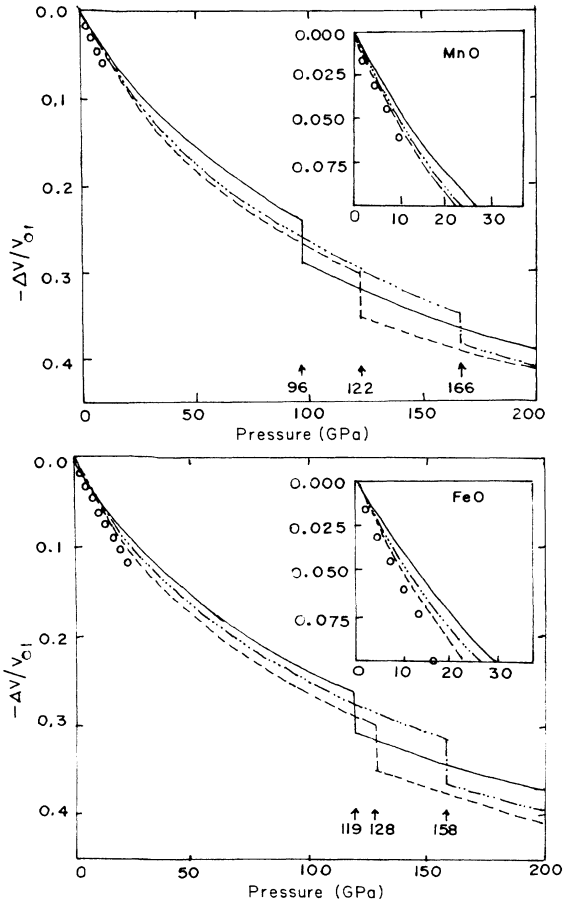

FIG. 3. Phase diagram of MnO and FeO. Other notations are same as in Fig. 1. Experimental points (○) are taken from Ref. 42.

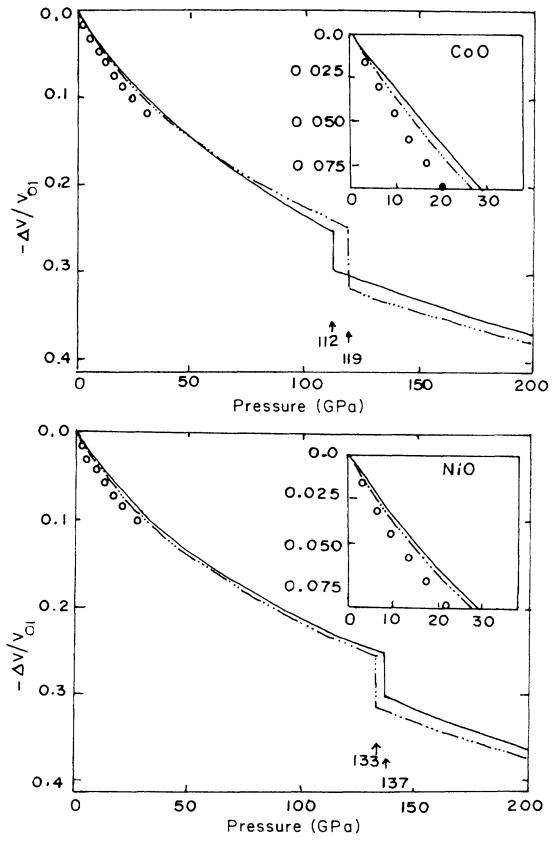

FIG. 4. Phase diagram of CoO and NiO. Other notations are same as in Fig. 1. Experimental points (○) are taken from Ref. 42.

the DMO are plotted in Figs. 1—4. For a meaningful visual comparison of the merits of different models to predict the experimental data in the low-pressure region (0—30 GPa) we have plotted them separately in the above-mentioned figures.

The pressure variations of second-order elastic (SOE) constants of DMO in NaCl phase, obtained from TBP model have been presented in Figs. 5—12. The required expressions for the SOE constants appropriate for the present three body potential are given below for NaCl phase:

$$C_{11}=\frac{e^2}{4r_0^4}[-5.112Z_m^2+A_{12}+\tfrac{1}{2}(A_{11}+A_{22}+B_{11}+B_{22}) +9.3204Zr_0f'(r_0)]\,, \quad (2)$$

$$C_{12}=\frac{e^2}{4r_0^4}[0.226Z_m^2-B_{12}+\tfrac{1}{4}(A_{11}+A_{22}-5B_{11}-5B_{22}) +9.3204Zr_0f'(r_0)]\,, \quad (3)$$

$$C_{44}=\frac{e^2}{4r_0^4}[2.556Z_m^2+B_{12}+\tfrac{1}{4}(A_{11}+A_{22}+3B_{11}+3B_{22})]\,, \quad (4)$$

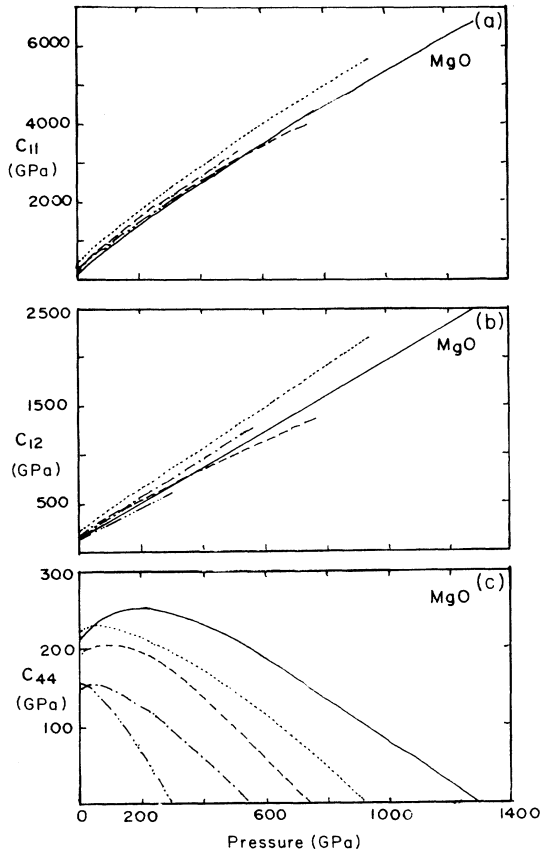

FIG. 5. Variation of elastic constants with pressure for MgO. (a) C_{11}, (b) C_{12}, (c) C_{44}. Other notations are defined in Fig. 1.

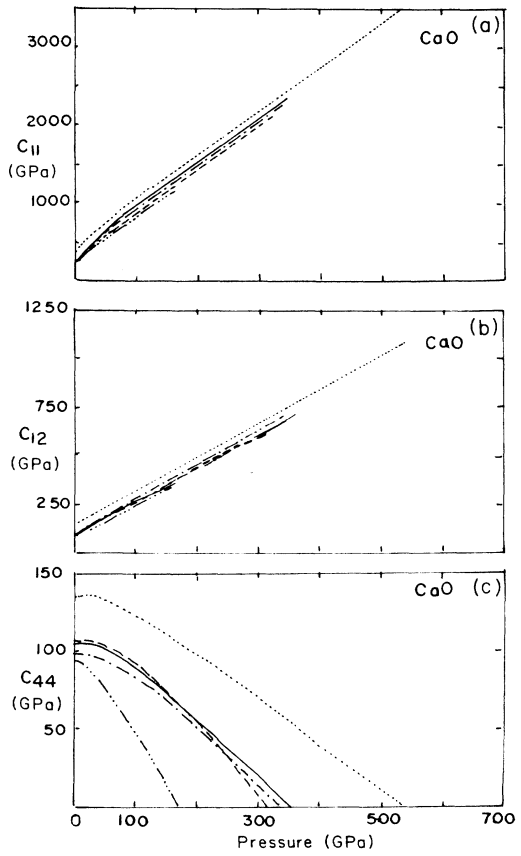

FIG. 6. Variation of elastic constants with pressure for CaO. (a) C_{11}, (b) C_{12}, (c) C_{44}. Other notations are defined in Fig. 1.

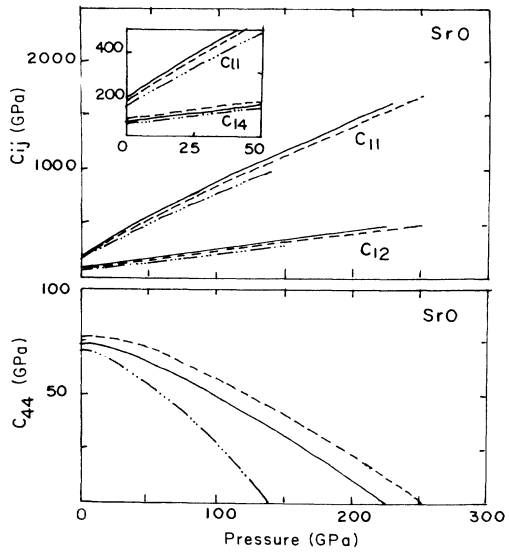

FIG. 7. Variation of elastic constants with pressure for SrO. Upper panel: C_{11} and C_{12}; lower panel: C_{44}. Other notations are defined in Fig. 1.

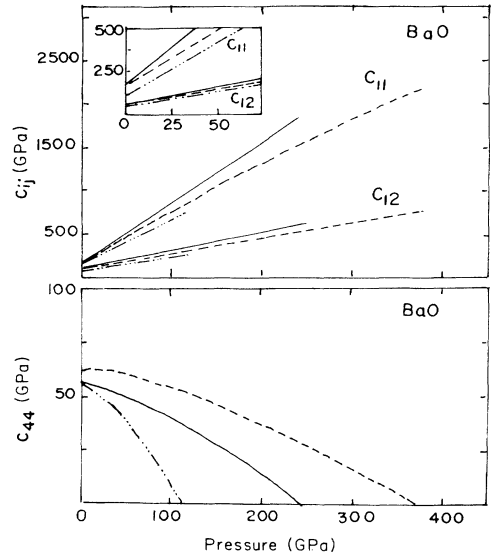

FIG. 8. Same as in Fig. 7 for BaO.

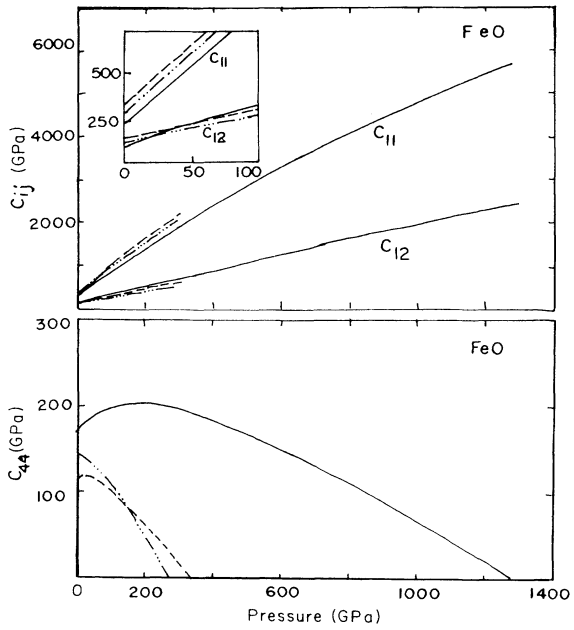

FIG. 10. Same as in Fig. 7 for FeO.

where A_{ij} and B_{ij} are short-range force constants, as defined by Singh and Chandra.[25] The appropriate values of r_0, the near-neighbor separations appearing in the above expressions and those for A_{ij} and B_{ij} are obtained by minimizing the Gibbs free energy of the B_1 phase at various pressures. The high-pressure experimental values of SOE constants for DMO are not available and hence the results of the present model could be compared graphically only with other theoretical predictions in Figs. 5—12.

The pressure derivatives of SOE constants at zero pressure are critical parameters that govern the high-pressure behavior of these oxides and are of considerable interest in geophysical studies[26] of the earth's mantle. We have, therefore, calculated their values and reported in Table IV and compared with experimental and other theoretical results. In our earlier paper,[1] we have presented the results of the pressure derivatives obtained by the method of finite difference approximation for the SOE constants in 0—1 GPa range. In this paper we have used the expressions for these derivatives given by Singh[18] which are

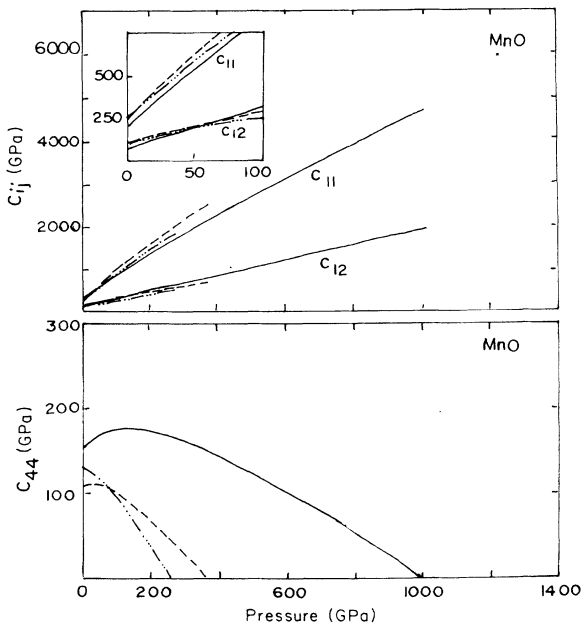

FIG. 9. Same as in Fig. 7 for MnO.

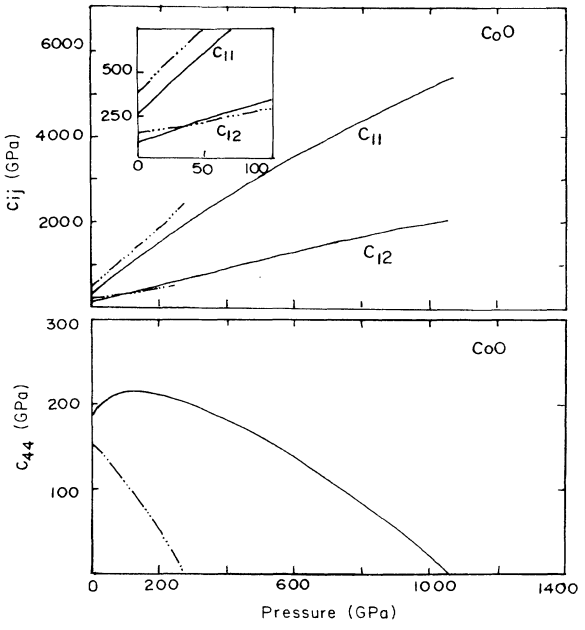

FIG. 11. Same as in Fig. 7 for CoO.

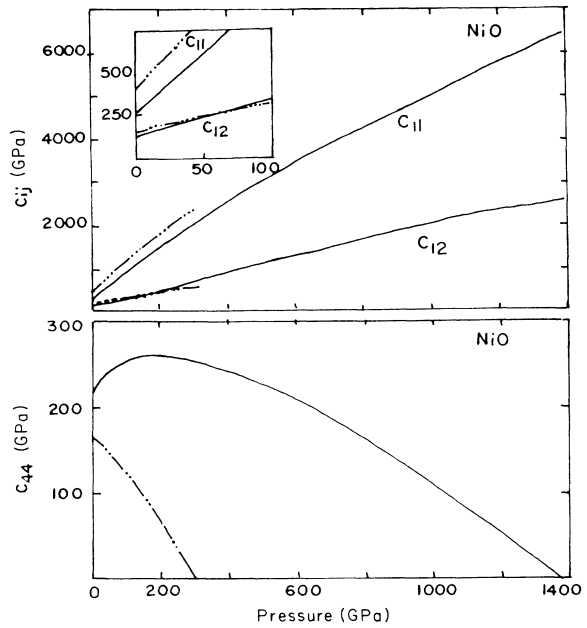

FIG. 12. Same as in Fig. 7 for NiO.

more appropriate for present calculations. The pressure derivatives of SOE constants are expressed as

$$(dC_{44}/dP)=Q^{-1}[-11.389Z_m^2-A_1+3B_1 -\tfrac{1}{4}(C_2+2A_2-10B_2) -44.652Zr_0f'(r_0)]\ , \quad (5)$$

$$(dB/dP)=Q^{-1}[-4.658Z_m^2+A_1+A_2-\tfrac{1}{3}(C_1+C_2) +55.921Zr_0f'(r_0)-13.980Zr_0^2f''(r_0)]\ , \quad (6)$$

$$(dC/dP)=Q^{-1}[-11.838Z_m^2-\tfrac{1}{2}C_1-\tfrac{1}{8}(C_2+6A_2-6B_2) +25.537Zr_0f'(r_0)-6.990Zr_0^2f''(r_0)]\ , \quad (7)$$

where

$$Q=-2.330Z_m^2+A_1+A_2+27.961Zr_0f'(r_0)$$

and

$$B=\tfrac{1}{3}(C_{11}+2C_{12});\quad C=\tfrac{1}{2}(C_{11}-C_{12})\ .$$

A_i, B_i, and C_i are the short-range force constants, defined in Ref. 18. The calculated values of pressure derivatives of SOE constants have been presented in Table IV and compared with the available experimental and other theoretical results.[27,37]

IV. RESULTS AND DISCUSSIONS

It is obvious from Table III that the present TBP model has correctly predicted the relative stability of competitive structures as the values of ΔU are positive in all cases. It is also interesting to note that the magnitudes of ΔU obtained from our TBP model are nearly the same as those obtained from other theoretical models[1,4,5] in all DMO, except for MnO. A look at Table III also shows that the values of the phase transition pressure (P_t) obtained from our TBP model are generally closer to available experimental data.[12,15,24] In case of MgO, the higher value of P_t obtained from TBP is mainly due to the three-body interactions and this is in keeping with the trends shown by the results obtained from MEG (YA) model[4] and recent calculations made by Chang and Cohen[5] from local-density theory and Mehl *et al.*[9] from LAPW method, which also explicitly contains many-body interactions. It is seen from Fig. 1 that the static compression curves for MgO obtained from models I and II and present TBP are identical at low pressures and they show deviation from the experimental data at room temperature.[13,41] On the other hand, the compression curves calculated by Hemley *et al.*[11] (not shown in Fig. 1) incorporating the temperature effects in the electron gas model give better agreement with experimental data[13,41] at room temperature. It is obvious from Table III that our TBP results have yielded better predictions of B_1-B_2 transition pressure for MgO, CaO, and SrO than those achieved from MEG (YA) (Ref. 4) and LDT (Ref. 5) models. However, our TBP results on them are still larger in magnitude by about 50 GPa in CaO and SrO and over 150 GPa in MgO than their corresponding experimental values.[10,15,24] This might be due to the pronounced effects of three-body interactions (TBI) in these solids. It is, however, interesting to note that the TBP results on P_t for SrO and FeO have shown better agreement than those obtained by us[1] without making use of TBI effects.

The relative volume changes of 4.4% at the transition pressure predicted from the present model are in good agreement with its experimental value of 4% in FeO.[24] The predictions of relative volume change for other oxides in this respect are, however, lower from the present model as compared to those obtained from earlier models.[1] Compression curves in the low pressure range show that MEG (Wat) model,[4] is superior in case of MgO and CaO but the present model predictions are comparable with other models and hence we may conclude that TBI effects have not shown any marked improvement in this respect.

The pressure variations of SOE constants, shown graphically in Figs. 5 to 12 shows that the general trends is maintained by the present TBP model. However, a significant increase in the value of shear instability is predicted by the TBP in case of MgO and transition metal oxides. For MgO, this trend of predicting very high values of shear instability (1310 GPa) is consistent with the high values (1050 GPa) of P_t, predicted by LDT.[5] This can be considered interesting as the value of shear instability should always be more than the transition pressure and the present model in this respect has shown improvement and provided support to the prediction achieved from LDT pseudopotential model for MgO. The successful predictions achieved from the present model in MgO and CaO can be considered remarkable in view of the fact that it has considered overlap repulsion

TABLE IV. Pressure derivatives of second-order elastic constants of divalent metal oxides.

Crystals	Models	$\frac{dC_{44}}{dP}$	$\frac{dB}{dP}$	$\frac{dC}{dP}$	Reference
MgO	TBP	1.50	2.87	1.68	present
	I	−0.12	3.85	2.96	38
	II	0.78	4.75	2.89	38
	MEG (YA)	0.43	4.21	2.67[a]	4
	MEG (Wat)	0.41	4.02	2.41[a]	4
	Expt.	1.12±0.06[b]	4.29±0.08[b]	3.67[c]	
CaO	TBP	0.41	3.44	2.65	present
	I	−0.10	3.90	2.99	38
	II	0.38	4.45	3.08	38
	MEG (YA)	0.17	4.25	3.12[a]	4
	MEG (Wat)	0.19	4.09	2.85[a]	4
	Expt.	0.60±0.1[c]	4.8±0.1[d]	3.40±0.8[c]	
SrO	TBP	0.20	3.47	2.90	present
	I	−0.06	3.84	2.94	38
	II	0.24	4.38	3.20	38
	Expt.	−0.02[e]	~4.4[f]	4.00[c]	
BaO	TBP	−0.05	3.59	2.91	present
	I	−0.02	3.78	2.70	38
	II	0.30	4.42	3.16	38
MnO	TBP	1.60	3.21	2.18	present
	I	−0.07	3.82	2.84	38
	II	0.30	4.55	3.36	38
FeO	TBP	1.67	3.28	2.10	present
	I	−0.11	3.88	2.99	38
	II	+0.27	4.60	3.46	38
	Expt.		3.20±0.3		24
CoO	TBP	1.63	3.34	2.35	present
	I	−0.20	4.06	3.39	38
NiO	TBP	1.81	3.24	2.03	present
	I	−0.20	4.06	3.37	38

[a]Obtained from Ref. 4 using $C=\frac{1}{2}(C_{11}-C_{12})$.
[b]Reference 39.
[c]Reference 28.
[d]Reference 32.
[e]Reference 39.
[f]Reference 40.

effective only up to second neighbors while MEG (Ref. 4) model considered it up to fourth-neighbor ions.

The pressure derivatives of SOE constants presented in Table IV show that the values of dC_{44}/dP obtained from TBP model are in better agreement with their available experimental data[29,39] than those achieved from MEG models.[4] However, the predictions of dB/dP and dC/dP obtained from TBP model is not so good as those revealed by MEG models.[4] This might be due to the exclusion of short-range higher-neighbor interaction effects, which play an important role in such predictions.

Finally, we may conclude that the simple three body potential model has yielded somewhat more realistic predictions of the phase transition and high-pressure behavior of the alkaline earth and transition metal oxides as compared to those achieved from the relatively more sophisticated models based on microscopic approach. The inclusion of three-body interactions has improved the prediction of phase-transition pressures over that obtained from the two-body potentials. Except for the higher values of the shear instability predicted by the present TBP model in some oxides, there is no marked changes in the predictions of the high-pressure elastic behaviors. The use of a suitable functional form for three-body force parameter $f(r)$, instead of using it as a structure independent model parameter, might improve the usefulness of the present model for estimating the actual high-pressure behavior of divalent metal oxides.

ACKNOWLEDGMENTS

The authors are thankful to the University Grants Commission for financial assistance and to Dr. B. K. Godwal for fruitful discussions.

*Present address: Max-Planck-Institut für Festkörperforschung, Heisenbergstrasse 1, Stuttgart 80, Federal Republic of Germany

[1]K. N. Jog, R. K. Singh, and S. P. Sanyal, Phys. Rev. B 31, 6047 (1985).
[2]M. J. L. Sangster and A. M. Stoneham Atomic Energy Research Establishment (Harwell) Report TP833 (1980) (unpublished).

[3]W. C. Mackrodt and R. F. Stewart, J. Phys. C **12**, 431 (1979).
[4]A. J. Cohen and R. G. Gordon, Phys. Rev. B **14**, 4593 (1976).
[5]K. J. Chang and M. L. Cohen, Phys. Rev. B **30**, 4774 (1984).
[6]M. L. Cohen and V. Heine, Solid State Phys. **24**, 37 (1970).
[7]D. Hohenberg and W. Kohn, Phys. Rev. **136**, B864 (1964); W. Köhn and L. J. Sham, Phys. Rev. **140**, A1133 (1965).
[8]R. K. Singh and S. P. Sanyal, Phys. Status Solidi B **113**, K23 (1982).
[9]M. J. Mehl, L. L. Boyer, and H. K. Krakauer, Bull. Am. Phys. Soc. **31**, 496 (1986).
[10]X. Bukowinski, Geophys. Res. Lett. **12**, 536 (1985).
[11]R. J. Hemley, M. D. Jackson, and R. G. Gordon, Geophys. Res. Lett. **12**, 247 (1985).
[12]W. J. Carter, S. P. Marsh, J. N. Frity, and R. G. McQueen, in *Accurate Characterization of the High-Pressure Environment*, edited by E. C. Lloyd, Natl. Bur. Stand. (U.S.) Circ. No. 326 (U.S. GPO, Washington, D.C., 1971), p. 147.
[13]H. K. Mao and P. M. Bell, J. Geophys. Res. **84**, 4533 (1979).
[14]C. W. Muhlhansen and R. G. Gordon, Phys. Rev. B **23**, 900 (1981).
[15]Y. Sato and R. Jeanloz, J. Geophys. Res. **86**, 11773 (1981).
[16]R. Jeanloz and T. J. Ahrens, H. K. Mao, and P. M. Bell, Science **206**, 829 (1979).
[17]A. J. Cohen and R. G. Gordon, Phys. Rev. B **12**, 3228 (1975).
[18]R. K. Singh, Phys. Rep. **85**, 259 (1982).
[19]R. K. Singh and S. P. Sanyal, Physica **132B**, 201 (1985).
[20]S. O. Lündqvist, Ark. Fys. **9**, 435 (1955); **12**, 263 (1957).
[21]P. O. Löwdin, Ark. Mat. Astron. Fys. **35A**, 30 (1947).
[22]D. W. Hafemiester and W. H. Flygare, J. Chem. Phys. **43**, 795 (1965).
[23]J. C. Slater and J. G. Kirkwood, Phys. Rev. **37**, 682 (1937).
[24]R. Jeanloz and T. J. Ahrens, Geophys. J. R. Astron. Soc. **62**, 505 (1980).
[25]R. K. Singh and K. Chandra, Phys. Rev. B **14**, 2625 (1976).
[26]F. D. Stacez, *Physics of the Earth* (Wiley, New York, 1969).
[27]J. Yamashita and S. Asano, J. Phys. Soc. Jpn. **28**, 1143 (1970).
[28]D. H-Chung, Philos. Mag. **8**, 833 (1963).
[29]R. W. G. Wyckoff, *Crystal Structures* (Wiley, New York, 1963), Vol. 1.
[30]A. L. Drago and I. L. Spain, J. Phys. Chem. Solids **38**, 705 (1977).
[31]R. A. Bartels and P. R. Son, Bull. Am. Phys. Soc. **16**, 357 (1971).
[32]Z. P. Chang and E. K. Craham, J. Phys. Chem. Solids **38**, 1355 (1977).
[33]V. H. Vetler and R. A. Bartels, J. Phys. Chem. Solids **34**, 1449 (1973).
[34]D. W. Oliver, J. Appl. Phys. **40**, 893 (1969).
[35]G. Kugel, C. Carabatos, B. Hennion, B. Prevot, A. Revcolevschi, and D. Tocchetti, Phys. Rev. B **16**, 378 (1977).
[36]N. Vchida and S. Saito, J. Acoust. Soc. Am. **51**, 1602 (1971).
[37]R. Watson, Phys. Rev. **111**, 1108 (1958).
[38]K. N. Jog, S. P. Sanyal, and R. K. Singh, Phys. Status Solidi A **91**, 45 (1985).
[39]P. R. Son and R. A. Bartels, J. Phys. Chem. Solids **33**, 819 (1972).
[40]L. G. Liv and W. A. Bassett, J. Geo. Phys. Res. **78**, 8470 (1973).
[41]E. A. Perez-Albuerne and H. G. Drickmer, J. Chem. Phys. **43**, 1381 (1965).
[42]H. G. Drickamer, R. W. Lynch, R. L. Clendenen, and E. A. Perez-Albuerne, Solid State Phys. **19**, 135 (1966).